Universitat de València — Facultat de Física

Máster en Física Avanzada

Especialidad en Física Teórica

Trabajo Fin de Máster

Zeros of the $W_L\, Z_L \rightarrow W_L\, Z_L$ amplitude: vector resonances at the LHC

Madeleine Adrien

Tutor: Jorge Portolés Ibáñez

Curso académico 2016/17

Table of Contents

1 Introduction

The spontaneous breaking of gauge symmetry is an essential feature of particle physics, in that it brings mass to the gauge bosons $W^{\pm}$ and Z and fermions and more broadly holds a very important place in our understanding of the Universe. The existence of a Higgs sector to explain it has been considered almost as early on as the inception of the Standard Model. It is very successful in explaining the experimental results. However, in 2000, the LEP experiment closed and no Higgs had yet been discovered. Scientists thus started to investigate new sectors that could break the electroweak symmetry and substitute for the Higgs physics.

One of the possibilities was the existence of a new strong sector that, through the non-linear sigma model, would spontaneously break the chiral symmetry $SU(2)_L \otimes SU(2)_R \to SU(2)_{L+R}$, with the electroweak symmetry being gauged. The experimentally-observed gauge bosons would receive mass with that mechanism [1, 2]. Actually, when an effective field theory is built for this model, one obtains the Chiral Perturbation Theory (ChPT) lagrangian, with the Goldstone bosons given by the spontaneous chiral symmetry breaking instead of the pions, and a change of scale and of Low Energy Constants (LECs). This theory is named the Effective Chiral Electroweak Theory (EChET), and as ChPT, it is a low-energy theory perturbative in momentum p, that is renormalizable order by order in its expansion. Moreover, so as to reproduce the physics of the Higgs sector, the constant $v = \frac{1}{\sqrt{\sqrt{2}\,G_F}} \simeq 246$ GeV, which is the vacuum expectation value of the Higgs, was introduced. EChET is a theory only valid at low energies compared to the theory scale $\Lambda_{EW} = 4\,\pi\,v \simeq 3$ TeV.

However, since the Higgs was discovered at the LHC in 2012, it has to be included in every model at energies $E \geq 0.1\ \mathrm{TeV} \simeq M_H$. The effective theory based on the non-linear sigma model can be modified so as to include the Higgs field. Despite the existence of this boson, we have no reason to exclude the possibility of a strong interacting sector at $E \sim 1$ TeV.

Furthermore, this strong sector predicts the existence of resonances, which the CMS and ATLAS experiments are currently searching evidence on. In effective theories such as EChET, the information on heavier resonances is found in the coupling constants. The main objective of this study is to investigate the spin 1 resonances at $E \sim 1$ TeV by analyzing the order four EChET scattering amplitude of $W_L Z_L \to W_L Z_L$. However, we know that the effective electroweak theory may not be valid at energies of the order of the TeV. Therefore, in order to use it to search for resonances, we have to employ a method to increase its validity range. Several of them exist, but we choose to take advantage of the smoothness of the zero contour of the EChET amplitudes. This method is only valid for resonances of spin $J \geq 1$, as we will explain in section 2.2.2.

Additionally, we decided to first test our method by searching for the $\rho(770)$ resonance using the ChPT amplitude of the $\pi^-\pi^0 \to \pi^-\pi^0$ scattering. The validity range of ChPT consists of energies up to $E \ll 4\,\pi f_\pi \simeq 1.16$ GeV, so the framework would not normally suffice in order to find the $\rho(770)$ resonance. That is where our Legendre zeros method can help. This particular resonance is already known, and the chiral theory has already been studied abundantly. We know that the coupling constants involved in our amplitude are saturated by vector resonances, and they have been measured. We will show that the result obtained with our technique indeed matches the $\rho(770)$ resonance. This validates its efficiency in finding vector resonances using low-energy theories. Moreover, the zeros method will provide us with a unitarization procedure for the scattering.

Then, we will apply the technique to the much less known electroweak case, where we assume that the coupling constants are also saturated by the vector resonances. The LECs have not yet been measured, neither has any resonance at these energies, so any information that our method can unveil is welcome. We will look for resonances that are involved in the $W_L Z_L \to W_L Z_L$

scattering. Two theoretical points will make our calculation of the amplitude possible. First, the equivalence theorem, that relates the $W_L Z_L \to W_L Z_L$ amplitude with the scattering one of the corresponding Goldstone bosons from this electroweak strong sector. This theorem is only valid at energies $E \gg M_W \sim 0.1$ TeV, and was originally intended for an intermediate study of our targeted scattering amplitude with a very heavy Higgs. The second point is the link that exists between ChPT and EChET. That will make our calculation of the Goldstone boson amplitude considerably easier, as we can thus use the existing work done on the $\pi^-\pi^0 \to \pi^-\pi^0$ chiral amplitude (π being the pion here). Then, we will apply our Legendre zeros method to the effective electroweak amplitude so as to extend the validity range of the theory. Finally will come the deduction of the minimum allowed resonance mass as a function of the LECs involved in the amplitude.

The outline of this study is the following. First, section 2.1 reviews the main points of the Chiral Perturbation Theory. The following section develops the Legendre zeros method using the example of the pion pion scattering $\pi^-\pi^0 \to \pi^-\pi^0$. The resonance mass will be derived, and so will a unitarization procedure of the amplitude based on the zero contour. Section 2.3 comments on the change in our results with the addition of the $O(p^6)$ corrections (as all the previous calculations were done at $O(p^4)$). Then, section 3.1 focuses on the equivalence theorem, which enables us to calculate our scattering amplitude $A(W_L Z_L \to W_L Z_L)$ using the electroweak effective theory. The following section will introduce the lagrangian L_{EChET} of this effective theory, and section 3.3 calculates the $O(p^4)$ amplitude of the $W_L Z_L \to W_L Z_L$ scattering using the results from the two previous sections. Ultimately, section 3.4 focuses on applying the zeros method to this case and on deriving two figures of the minimum allowed resonance mass as a function of the coupling constants. The Higgsless case will be considered as well as the one including the Higgs field, for comparison. We will end with a brief review of other methods developed to search for vector resonances at $E \sim 1$ TeV, and we will comment on the latest experimental results on the matter.

2 Pions case : Study of $\pi^-\pi^0 \to \pi^-\pi^0$

2.1 The Chiral Perturbation Theory framework

2.1.1 Spontaneous Chiral Symmetry Breaking

In the absence of external currents and neglecting the quark masses, the theory of strong interactions is commonly described by the following lagrangian [3] :

$$L^0_{\mathrm{QCD}} = -\frac{1}{4} G^a_{\mu\nu} G^{\mu\nu}_a + i\overline{q_L}\gamma^\mu D_\mu q_L + +i\overline{q_R}\gamma^\mu D_\mu q_R. \tag{1}$$

This lagrangian is invariant in flavour space under the group $G \equiv SU(N_f)_L \otimes SU(N_f)_R = SU(N_f)_{L+R=V} \otimes SU(N_f)_{R-L=A}$. This is called Chiral Symmetry, and it is a global one. We will consider in this subsection $N_f = 3$ flavours for the quarks : u,d and s. This symmetry defines two sets of Noether currents $J^{a\mu}_X = \frac{1}{2}\overline{q_X}\gamma^\mu \lambda^a q_X$, where $X = L, R$ and the λ^a are the Gell-Mann matrices. There are also two conserved charges Q^a_L and Q^a_R, with $Q^a_X = \int d^3x J^{a0}_X(x)$. Using the vector and axial vector notations, it gives us $Q^a_V = Q^a_L + Q^a_R$ and $Q^a_A = Q^a_R - Q^a_L$.

However, at low energies, the running QCD coupling constant α_s becomes large. The quarks are thus not the appropriate degrees of freedom to be working with then, the hadrons are. Although some of the hadrons observed can be classified in $SU(3)_V$, none can be found to be axial vector. Moreover, there are 8 very light pseudoscalar mesons observed in nature which can be explained theoretically as Goldstone bosons. That indicates that the 8 generators of $SU(3)_A$ are spontaneously broken when changing the degrees of freedom from the quarks to the hadrons in the lagrangian. We can also express that using the conserved charges and the hadronic vacuum $|0\rangle$:

$$\forall a, \quad Q_V^a|0\rangle = 0 \;\text{ and }\; Q_A^a|0\rangle \neq 0. \tag{2}$$

Having $Q_A^a|0\rangle \neq 0$ makes it possible for an operator O^a to exist such that $\langle 0|[Q_A^a, O^a]|O\rangle \neq 0$. And indeed, with $O^a = \overline{q}\gamma_5\lambda^a q$, we have :

$$\langle 0|[Q_A^a, O^a]|O\rangle = -\frac{1}{2}\langle 0|\overline{q}\{\lambda^a, \lambda^a\}q|0\rangle = -\frac{2}{3}\langle 0|\overline{q}q|0\rangle \neq 0. \tag{3}$$

According to Goldstone's theorem (1961), there is thus one massless Goldstone boson $|G^a\rangle$ for each broken generator Q_A^a of $SU(3)_A$, which means that we have just introduced 8 massless Goldstone bosons into the theory. As we explained, these were identified with the octet of pseudoscalar particles (π^-, π^0, π^+, K^-, K^+, K^0, $\overline{K^0}$, η), which are the lightest mesons. As $\langle 0|[Q_A^a, O^a]|O\rangle$ has the quantum numbers of the vacuum, it is a scalar. Strong interactions conserve parity, so $[Q_A^a, O^a]$ has to be a scalar as well. Since parity transforms Q_A^a into $-Q_A^a$, we can deduce that the O^a have to be pseudoscalar operators, and that the $|G^a\rangle$ indeed result in being pseudoscalar particles, as expected by the experiment. In the end, the eight pseudoscalar mesons do have a small mass given by the quark-mass matrix which when added, breaks explicitly chiral symmetry.

2.1.2 Building an effective field theory

2.1.2.1 The reasons. At high energies, asymptotic freedom is observed and the running QCD coupling constant α_s is small. The spectrum of particles observed is thus composed of quarks, and perturbation theory can be applied with good results. At low energies however, the running QCD coupling constant is very large, and the situation is different. As the interactions between quarks and gluons are strong, these are confined and not observed as such. The spectrum is instead made of hadrons. It would therefore be more accurate to make a theoretical description of the interactions in terms of these hadrons, but the task is enormous due to the immense variety of them. We thus find ourselves in a sort of impasse. However, an important simplification of the situation can be made at very low energies : there is a mass gap between the above-mentionned pseudoscalar octet of mesons, and the following particles on a mass scale, the $\rho(770)$ resonance being the lightest one of them [1] :

$$M_\pi \simeq 140 \text{ MeV} \;\text{ and }\; M_{K,\eta} \leq 550 \text{ MeV}, \quad \text{whereas} \;\; M_\rho \simeq 770 \text{ MeV}. \tag{4}$$

Therefore, an effective field theory can be built, using as only degrees of freedom the eight light pseudoscalar mesons, and taking into account the chiral symmetry that our QCD lagrangian in Eq.(1) displays. This theory will understandably only be accurate under a certain energy scale Λ. It is called the Chiral Perturbation Theory. Actually, the heavier degrees of freedom that nature has to offer were integrated out of the action in order to obtain this low-energy formulation. However, the information corresponding to them was not lost. It remains contained in the often undetermined constants of the effective lagrangian. This new theory will not only make calculations considerably easier and faster, but it will also enable us to compute scattering amplitudes in a systematic and rigorous way, with each higher order a smaller correction to the lower ones.

2.1.2.2 The principles. Firstly, as we said, the Goldstone bosons should be the only degrees of freedom of this theory. Thus, we need a way to parametrize them. We will work with $N_f = 2$ flavours from here on. Chiral symmetry is spontaneously broken in the hadronic spectrum. Therefore, in order to implement it at the Goldstone bosons level, we have to consider a non-linear representation of these particles :

$$U(\phi) = \exp\left[i\,\frac{\sqrt{2}}{f}\,\Phi\right], \quad \text{where} \quad \Phi = \frac{\tau^a}{\sqrt{2}}\cdot\phi^a = \begin{pmatrix} \frac{1}{\sqrt{2}}\pi^0 & \pi^+ \\ \pi^- & -\frac{1}{\sqrt{2}}\pi^0 \end{pmatrix} \tag{5}$$

1. The mass gap is a lot bigger (and a more accurate concept) in $SU(2)$, where the K and η are not considered.

where τ^a, $a = 1, 2, 3$ are the Pauli matrices. $U(\phi)$ transforms under the chiral group $G \equiv SU(2)_L \otimes SU(2)_R$ in the following way :

$$U(\phi) \xrightarrow{G} g_R\, U(\phi)\, g_L^\dagger\,, \quad \text{where} \quad (g_L\,,\, g_R) \in G\,. \tag{6}$$

As we are working at low energies, it is particularly interesting to arrange the effective lagrangian in terms of increasing powers of momentum p_μ, or which is the same, in terms having an increasing number of derivatives ∂_μ. Then, we will be able to treat calculations perturbatively, and the terms that have the lowest number of derivatives will dominate.

Building the effective lagrangian consists in finding the most general lagrangian there is which would also be invariant under chiral symmetry and parity transformations. Indeed, as strong interactions conserve parity, any effective theory of them will also conserve it. We know that parity P transforms $p^\mu = (p^0,\ \vec{p}) \xrightarrow{P} (p^0,\ -\vec{p})$. Hence, we conclude that for our lagrangian to be invariant under parity transformations and Lorentz invariance, it has to contain only even powers of momenta, which also means only even numbers of derivatives. We will write $L_{ChPT} = \sum_n L_{2n}$.

2.1.3 Chiral Perturbation Theory at lowest order

We will set out to investigate the effective lagrangian at lowest order (in momentum). Since $UU^\dagger = I$, there is no non-trivial zero-order lagrangian. Indeed, to be chirally invariant, L_0 can only display $\langle UU^\dagger\rangle$ (where $\langle..\rangle$ denotes the trace in the flavour space of the matrix inside). The second order is thus the lowest one in our study. The most general chiral invariant lagrangian at $O(p^2)$ has the following expression [3] :

$$L_2 = \frac{f^2}{4}\, \langle \partial_\mu U^\dagger\, \partial^\mu U\rangle. \tag{7}$$

Performing calculations at $O(p^2)$ in Chiral Perturbation Theory consists in accounting only for the order-two chiral lagrangian at tree level. It is possible, using Eq.(5), to develop L_2 into a power series of Φ. Then, we observe a kinetic term in Φ, as well as an infinite number of interactions, between increasing numbers of Goldstone bosons. It is the requirement that this kinetic term be properly normalized that fixes the coupling constant of L_2 to $\frac{f^2}{4}$. It is now thus possible to calculate scattering amplitudes of processes involving any number of Goldstone bosons, at lowest order in momentum and with just one coupling constant f.

Moreover, there also exists an extended lagrangian of QCD, involving couplings of the mesons fields to external classical fields v_μ (vector), a_μ (axial vector), s (scalar) and p (pseudo-scalar) :

$$L_{\rm QCD} = L^0_{\rm QCD} + \overline{q}\, \gamma^\mu (v_\mu + \gamma_5 a_\mu)\, q - \overline{q}\, (s - i\gamma_5 p)\, q. \tag{8}$$

One of the assets of this new extended QCD lagrangian is that it enables us to introduce the electromagnetic and weak interactions, and the explicit breaking of chiral symmetry into L_{QCD}. In order to do that, we would take :

$$\begin{aligned} & r_\mu \equiv v_\mu + a_\mu = e\, QA_\mu \\ \text{and} \quad & l_\mu \equiv v_\mu - a_\mu = e\, QA_\mu + \frac{e}{\sqrt{2}\,\sin\theta_W}(W_\mu^\dagger T_+ + h.c.), \end{aligned} \tag{9}$$

where Q is the quark-charge matrix $Q = \begin{pmatrix} \frac{2}{3} & 0 \\ 0 & -\frac{1}{3} \end{pmatrix}$ and $T_+ = \begin{pmatrix} 0 & V_{ud} \\ 0 & 0 \end{pmatrix}$ displays the appropriate coefficients of the CKM matrix.

The symmetry conserved here is broader than the global chiral one that we used to have in Eq.(1). Thanks to the new external fields, our extended QCD lagrangian can be invariant under *local* chiral transformations :

$$\begin{aligned} & q_L \longrightarrow g_L q_L\,, && l_\mu \longrightarrow g_L\, l_\mu\, g_L^\dagger + i\, g_L\, (\partial_\mu\, g_L^\dagger)\,, \\ & q_R \longrightarrow g_R q_R\,, && r_\mu \longrightarrow g_R\, r_\mu\, g_R^\dagger + i\, g_R\, (\partial_\mu\, g_R^\dagger)\,, \\ \text{and} \quad & s+ip \longrightarrow g_R(s+ip)g_L^\dagger\,. && \end{aligned} \tag{10}$$

$$\text{where } (g_L,\, g_R) \in G' \equiv SU(3)_L \otimes SU(3)_R.$$

We are now naturally interested in building an effective field theory out of the extended QCD lagrangian of Eq.(8). In this case, the degrees of freedom of the theory are not only the Goldstone bosons, with their non-linear representation $U(\phi)$, but also the external classical fields v_μ, a_μ, $s+ip$ and $s-ip$. The symmetry that our effective lagrangian has to conserve now is the local chiral symmetry, as well as parity. It can be shown that the most general lagrangian fulfilling these conditions is the following one :

$$L_2 = \frac{f^2}{4}\, \langle (D_\mu U)^\dagger\, (D^\mu U) + U^\dagger \chi + \chi^\dagger U \rangle, \tag{11}$$

$$\begin{aligned} \text{where} \quad D_\mu U &= \partial_\mu U - i\, r_\mu U + i\, U\, l_\mu\,, \\ \chi &= 2\, B_0\, (s+ip). \end{aligned} \tag{12}$$

We see that B_0 is another coupling constant of our theory. The masses of the Goldstone bosons can be introduced through the scalar external field by taking :

$$s = M + \ldots\,, \quad \text{where } M \text{ is the quark-mass matrix } M = \begin{pmatrix} m_u & 0 \\ 0 & m_d \end{pmatrix}, \tag{13}$$

$$\text{so then} \quad \chi = 2\, B_0\, M + \ldots \simeq \begin{pmatrix} M_\pi^2 & 0 \\ 0 & M_\pi^2 \end{pmatrix} \quad \text{in the isospin limit.} \tag{14}$$

Moreover, if we develop the second and third terms of Eq.(11) as a power series of the Goldstone bosons fields using as s the quark-mass matrix as suggested after Eq.(8), and taking $p=0$ (as done in Eq.(15)), we can give mass to the Goldstone bosons. Their masses will naturally be expressed as functions of the quark masses, and that will give us a correspondence between them.

$$\frac{f^2}{4}\, \langle U^\dagger \chi + \chi^\dagger U \rangle = \frac{f^2}{4}\, 2B_0\, \langle M(U+U^\dagger) \rangle = B_0 \left(-\langle M\Phi^2 \rangle + O(\frac{\Phi^4}{f^2}) \right). \tag{15}$$

This is interesting, since as at low energies, no quarks can be observed, and that makes it rather difficult for us to measure their masses. On the other hand, our Goldstone bosons are perfectly observable at a range of energies attainable, so it is considerably easier for us to know their masses. Having a relation between the masses of the two enables us to derive information on the masses of quarks.

It is possible to calculate the Noether currents of the local chiral symmetry. From there, we can deduce the axial current $J_A^\mu = J_L^\mu - J_R^\mu$ in terms of the Goldstone bosons fields, and relate that expression to the definition of the pion decay constant :

$$\langle 0|\, (J_A^\mu)^{12}\, |\pi^+\rangle \;=\; i\, \sqrt{2}\, f_\pi\, p^\mu. \tag{16}$$

Ultimately, we see that the coupling constant f of the order-two lagrangians of Eq.(7) and Eq.(11) is actually the pion decay constant : $f = f_\pi \simeq 92.4\ \mathrm{MeV}$. With a similar reasoning, it is also possible to express the coupling constant B_0 as a function of the quark condensate :

$$\langle 0|\, \bar{q}^j q^i\, |0\rangle = -\, f^2 B_0\, \delta^{ij}. \tag{17}$$

2.1.4 Chiral Perturbation Theory at $O(p^4)$

In order to use Chiral Perturbation Theory at order four, three elements should be taken into account. First, all graphs based on L_4 at tree level. Second, all graphs based on L_2 at one-loop level, and finally, adding the chiral anomaly, which we will not discuss here.

L_4 is the most general lagrangian of order four conserving all the same symmetries as QCD, which we mentioned earlier in this work. Its detailed expression can be found in [4], and the part of it that we will use in this study is :

$$L_4 = \frac{l_1}{4}\langle (D^\mu U)^\dagger (D_\mu U)\rangle^2 + \frac{l_2}{4}\langle (D^\mu U)^\dagger (D^\nu U)\rangle \langle (D_\mu U)^\dagger (D_\nu U)\rangle + \dots . \tag{18}$$

It has 7 coupling constants l_i, which are accessible by measurement, and three more named h_i that are not directly measurable because they accompany terms that do not involve Goldstone bosons fields.

It is worth mentioning that it is possible to renormalize the divergent loops from L_2 with L_4. Indeed, if a regularization maintaining the symmetries of the lagrangian is chosen, then the counter-terms for the L_2 loops would have to conserve the same symmetries, and thus already be "included" in L_4 (as it has the most general expression possible). Then, we see the renormalized coupling constants of L_4 (the l_i^r's) appear.

We can also deduce the Chiral Perturbation Theory scale. With each loop comes a factor of $\frac{E^2}{(4\pi f_\pi)^2}$. An inherent concept to the low-energy expansion theory that is ChPT is that diagrams with loops, adding two additional powers of momentum, do not prevail compared to tree-level diagrams. In order for it to be consistent with the loop factor that we have just introduced, the energies we are working with should be $E \ll \Lambda_{ChPT} = 4\pi f_\pi \simeq 1.2\ \mathrm{GeV}$.

2.2 Uncovering resonances : Legendre zeros method

2.2.1 General principle

To start with, we are already familiar with the concept of deriving from a lagrangian L_R describing the coupling of resonances to our pseudoscalar fields an estimate of the chiral coupling constants $\overline{l_i}$ [5]. These expressions will be functions of the coupling constants of L_R and of the resonances masses. We will investigate whether the opposite method is also successful : we will study whether values of $\overline{l_i}$ obtained phenomenologically can accurately predict the mass of the resonance involved in the process under study.

However, the theory which enables us to perform calculations regarding our scattering process is the Chiral Perturbation one, and its validity range ends around 500 MeV. This value is well below the mass of the resonance that we know we have involved in the $\pi^-\pi^0 \to \pi^-\pi^0$ elastic scattering : the $\rho\,(770)$. There are different methods available to extend the validity region of results obtained with ChPT, some of which being resummation techniques such as Padé approximants, the N/D construction or also the inverse amplitude method [6, 7, 8].

The method that we study here is the Legendre zeros method [9]. We will derive the amplitude $F(s,t)$ of our process using ChPT. Then, we will study its zeros, because it was proven phenomenologically that its zero contour is smooth. This means that the relation obtained through $F(s,t) = 0$ will have a validity range beyond the 500 MeV of ChPT. It actually holds up to 900 MeV [10], which enables us to verify whether it predicts our resonance at 770 MeV. This relation, being obtained from $F(s,t)$, will contain information about the resonance through the coupling constants, which is exactly what we want.

The general idea behind this first section focusing on the $\pi^-\pi^0 \to \pi^-\pi^0$ scattering is to test the Legendre zeros method in a case already partly known (as we already know that the vector $\rho(770)$ is the only resonance involved in this process at such low energies). Then, we will apply the method to a case with a similar dynamics but which cannot be as "easily" investigated experimentally, in order to try to derive some information about it as well.

2.2.2 Legendre polynomials and partial waves

The scattering under study is $\pi^-(p_1)\,\pi^0(p_2) \to \pi^-(p_3)\,\pi^0(p_4)$. We will work here with the Mandelstam variables s, t and u. Their relations to the momenta of the particles are the following :

$$s = (p_1 + p_2)^2 \qquad \text{and} \qquad t = (p_1 - p_3)^2 = -\frac{1}{2}\,(s - 4M_\pi^2)\,(1 - z)\,. \tag{19}$$

where we have written $z \equiv \cos\theta$, θ being the angle between $\vec{p_1}$ and $\vec{p_3}$, and where M_π is the mass of the pions. We will work with the on-shell relation $s + t + u = 4M_\pi^2$, and considering all Mandelstam variables to be complex ones.

We will call $F(s,z)$ the scattering amplitude of our process. Using the isospin symmetry and Clebsch-Gordan coefficients, it can be shown that ($F^I(s,z)$ being the isospin defined amplitude) :

$$F(s,z) = \frac{1}{2}\,[\,F^1(s,z) + F^2(s,z)\,]. \tag{20}$$

A core step of our method is the decomposition of the isospin amplitudes into Legendre polynomials, in the s-channel :

$$F^I(s,z) = 32\pi \sum_{l=0}^{\infty} (2l+1)\; f_l^I\,(s)\; P_l\,(z). \tag{21}$$

This decomposition is meant to isolate one of the two variables s or t into the partial waves $f_l^I(s)$, and of course to introduce the Legendre polynomials $P_l\,(z)$. In addition, we will neglect the partial waves of angular momentum $l \geq 2$, as they give smaller contributions to the scattering amplitude than the lower-order $f_l^I\,(s)$ functions. It can be shown that for :

- $I = 1$: only the $l = 1$ contribution (the P-wave) exists.
- $I = 2$: only the $l = 0$ contribution (the S-wave) exists.

From phenomenology, we conclude that the isovector P-wave part dominates the amplitude, and that the exotic S-wave is significantly smaller.

Taking all of this into account and developing Eq. (20), we obtain :

$$F(s,z) = 16\pi\left(f_0^2\,(s) + 3\,z\,f_1^1\,(s)\right), \qquad \text{as } P_0(z) = 1 \text{ and } P_1(z) = z\,. \tag{22}$$

Moreover, we know that there is a vector resonance $\rho\,(770)$, whose mass we write M_ρ, that plays a role in the $\pi^-\pi^0$ elastic scattering. Therefore, at $s \sim M_\rho^2$, $f_1^1\,(s)$ is saturated by that resonance, and Eq.(22) thus becomes :

$$F(s,z) = 16\pi \left(f_0^2\,(s) + \frac{3}{\sigma}\, \frac{M_\rho\, \Gamma_\rho(s)}{M_\rho^2 - s - iM_\rho\, \Gamma_\rho(s)}\, z \right), \qquad \text{where } \sigma = \sqrt{1 - \frac{4M_\pi^2}{s}}\,. \tag{23}$$

Furthermore, we will use a formulation of the partial waves ensuring unitarity :

$$f_l^I\,(s) = \frac{1}{\sigma}\, e^{i\,\delta_l^I} \sin\,\delta_l^I\,, \tag{24}$$

where the $\delta_l^I\,(s)$ are the phase shifts of the partial waves.

As we explained, we are interested in the zeros of the scattering amplitude. From Eqs.(23) and (24), we calculate that :

$$\begin{aligned} F(s,z) = \frac{16\pi}{\sigma} \left(e^{i\,\delta_0^2} \sin\,\delta_0^2 + 3\, \frac{M_\rho\, \Gamma_\rho(s)}{M_\rho^2 - s - iM_\rho\, \Gamma_\rho(s)}\, z \right) \;=\; 0\,. \\ \Leftrightarrow\; 3\, \frac{M_\rho\, \Gamma_\rho(s)}{M_\rho^2 - s - iM_\rho\, \Gamma_\rho(s)}\, z = -\, e^{i\,\delta_0^2} \sin\,\delta_0^2\,. \\ \Leftrightarrow z = -\, \frac{e^{i\,\delta_0^2} \sin\,\delta_0^2}{3\; M_\rho\, \Gamma_\rho(s)}\, \Big(M_\rho^2 - s - iM_\rho\, \Gamma_\rho(s) \Big) \equiv z_0(s)\,. \end{aligned} \tag{25}$$

Then,

$$\begin{aligned} \mathrm{Re}\,(z_0(s)) &= -\, \frac{\cos\,\delta_0^2 \sin\,\delta_0^2}{3\; M_\rho\, \Gamma_\rho(s)}\, \Big(M_\rho^2 - s \Big) - \frac{\sin^2\,\delta_0^2}{3\; M_\rho\, \Gamma_\rho(s)}\; M_\rho\, \Gamma_\rho(s)\,. \\ &= -\, \frac{\sin\,2\delta_0^2}{6\; M_\rho\, \Gamma_\rho(s)}\, \Big(M_\rho^2 - s \Big) - \frac{1}{3}\, \sin^2\,\delta_0^2\,. \end{aligned} \tag{26}$$

The $I = 2,\; l = 0$ partial wave is exotic i.e. there is no resonance contributing to that partial wave. Since the imaginary part of the partial wave corresponds to the on-shell, observed part, and that there is nothing to observe for the $I = 2,\; l = 0$ wave, $|\mathrm{Im}\, f_0^2(s)| \ll |\mathrm{Re}\, f_0^2(s)|$. Therefore, using Eq.(24), we know that :

$$|\sin\,\delta_0^2| \ll |\cos\,\delta_0^2| \leq 1\,. \tag{27}$$

From the previous relationships, we get :

$$|\,\mathrm{Re}\,(z_0(M_\rho^2))\,| = \frac{1}{3}\, \sin^2\,\delta_0^2 \;\ll \frac{1}{3}\,. \tag{28}$$

We can thus conclude that when we have a single vector resonance saturating the P-wave and no particle in the S-wave, the resonance mass can be obtained as the solution of :

$$\mathrm{Re}\,(z_0(M_R^2)) \;\simeq\; 0\,. \tag{29}$$

We also notice that imposing $F(s,z)=0$ did not fix s nor z. Instead, it gave us a relation between the two variables : $z=z_0(s)$, $z_0(s)$ being a function of s. As we said so, s is still complex at that point. Once we have obtained the function $z_0(s)$, we define the zero contour as $\mathrm{Re}\,(z_0(s))$. Actually, what we do when we look for zeros of $F(s,z)$ as a function of the Legendre polynomials and around a resonance mass, is approximately look for the zeros of the Legendre polynomials themselves. Indeed, at that energy, minus the small contributions from the other partial waves,

$$F(s,z) \propto \;(2l_0+1)\; f_{l_0}^{I_0}\,(s)\; P_{l_0}\,(z), \tag{30}$$

I_0 and l_0 being the isospin and angular momentum of the resonance. The $f_{l_0}^{I_0}(s)$ shows a bump at the resonance, and the zeros of $P_{l_0}\,(z)$ create a dip in $F(s,z)$. A property of Legendre polynomials is that the number of zeros they have in the physical region $z\in[-1,1]$ is the value of l. Therefore, the number of dips (near-zeros) of $F(s,z)$ gives us the spin of the resonance.

Furthermore, it should be noticed that this Legendre zeros method only works for resonances of $l\geq 1$. It cannot be applied to scalar resonances as $P_0\,(z)=1$. Indeed, there would not be any z in the dominant term of the amplitude, so no $z=z_0(s)$-type relationship to derive. Since that relation is the central element of the method, we see that it cannot work in that case.

2.2.3 Obtaining M_R in practice

The amplitude at $O(p^4)$ of our scattering process was calculated in [4]. It is :

$$\begin{aligned} A\,(t,s,u) \;=\; & \frac{t-M_\pi^2}{f_\pi^2} \;+\; \frac{1}{6\,f_\pi^4}\Big[3\,(t^2-M_\pi^4)\,\bar{J}(t)+[\,s(s-u)-2\,M_\pi^2\,s+4\,M_\pi^2\,u-2\,M_\pi^4]\,\bar{J}(s) \\ & \qquad +[\,u(u-s)-2\,M_\pi^2\,u+4\,M_\pi^2\,s-2\,M_\pi^4]\,\bar{J}(u)\Big] \\ & +\frac{1}{96\,\pi^2 f_\pi^4}\left[2\left(\overline{l_1}-\frac{4}{3}\right)(t-2\,M_\pi^2)^2+\left(\overline{l_2}-\frac{5}{6}\right)(t^2+(s-u)^2)-12\,M_\pi^2\,t+15\,M_\pi^4\right], \end{aligned} \tag{31}$$

$$\begin{aligned} \text{where} \quad & f_\pi \simeq 92.4\text{ MeV is the pion decay constant,} \\ & M_\pi \simeq 138\text{ MeV is the mass of the pion,} \\ & \bar{J}(x)=\frac{1}{16\,\pi^2}\left(\sigma\; ln\left[\frac{\sigma-1}{\sigma+1}\right]+2\right) \\ \text{and} \quad & \sigma(x)=\sqrt{1-\frac{4M_\pi^2}{x}}. \end{aligned} \tag{32}$$

It can be noticed that $A(s,t,u)$ is symmetrical in its last two variables, so that $A\,(t,s,u)=A\,(t,u,s)$.

The $\overline{l_i}$ are connected to the renormalized $O(p^4)$ coupling constants through the following relations, where μ is the renormalization scale :

$$\begin{aligned} l_1^r(\mu) &= \frac{1}{96\,\pi^2}\left(\overline{l_1}\,+\,\ln\frac{M_\pi^2}{\mu^2}\right), \\ l_2^r(\mu) &= \frac{1}{48\,\pi^2}\left(\overline{l_2}\,+\,\ln\frac{M_\pi^2}{\mu^2}\right). \end{aligned} \tag{33}$$

However, it has been proven that the l_i^r are saturated by the lightest multiplet of vector resonances [5]. It is commonly accepted that consequently, the resonance contributions (once they have been integrated out from L_R) describe accurately the $l_i^r(\mu)$ for $\mu \simeq M_R^2$. These resonance contributions give :

$$\begin{aligned} l_1^r(\mu) &= -\frac{G_V^2}{M_V^2} - \frac{\nu_K}{24}, \\ l_2^r(\mu) &= \frac{G_V^2}{M_V^2} - \frac{\nu_K}{12}. \end{aligned} \tag{34}$$

where $M_V \simeq M_\rho$ is the mass of the lightest nonet of vector resonances, G_V is a coupling constant of the effective chiral resonance lagrangian L_R, and $\nu_K = \frac{1}{32\,\pi^2}\left(\ln\frac{M_K^2}{\mu^2}+1\right)$. Measurements teach us that $G_V \simeq 45$ MeV [11, 12]. From Eqs. (33) and (34), we compute :

$$\begin{aligned} \overline{l_1} &= -\ln\frac{M_\pi^2}{\mu^2} + 96\,\pi^2\left(-\frac{G_V^2}{M_V^2} - \frac{1}{768\,\pi^2}\left[\ln\frac{M_K^2}{\mu^2}+1\right]\right), \\ \overline{l_2} &= -\ln\frac{M_\pi^2}{\mu^2} + 48\,\pi^2\left(+\frac{G_V^2}{M_V^2} - \frac{1}{384\,\pi^2}\left[\ln\frac{M_K^2}{\mu^2}+1\right]\right). \end{aligned} \tag{35}$$

Therefore, taking $\mu = 0.77$ GeV, we calculate $\overline{l_1}$ and $\overline{l_2}$. We obtain :

$$\overline{l_1} = 0.25 \qquad \text{and} \qquad \overline{l_2} = 5.03\,. \tag{36}$$

With these values, we can compute M_ρ using the expression of $A(t,s,u)$ in Eq.(31), where we change u into a function of s and t using the on-shell relation, and then switching from the variables (s,t) to (s,z) with Eq.(19). Finally, we use the condition in Eq.(29) to calculate the resonance mass. The calculation was carried out with Mathematica. We obtained the function $z_0(s)$ using *FindRoot*. To derive the resonance mass, we also used *FindRoot*, but successively and on small intervals comprised between $\sqrt{s} \geq 0.2$ GeV (as the resonance has to be heavier than the pseudoscalars) and $\sqrt{s} \leq 1.16$ GeV (because above the chiral scale Λ_{ChPT}, even the relation obtained via the zero contour is not valid anymore).

We found $M_\rho = 0.75$ GeV, which is consistent with the knowledge we had of $M_\rho = 0.77$ GeV. This validates our method for vector resonances saturating the isovector P-wave in the absence of an exotic S-wave.

2.2.4 A unitarization procedure

As we mentioned, Eq.(24) ensures unitarity in our theory. However, as long as the phase shifts $\delta_l^I(s)$ are not properly defined, we cannot yet say that unitarity is satisfied. In this section, we will find an expression for $\delta_1^1(s)$ and use a parametrization for $\delta_0^2(s)$ developed by A. Schenk.

First, from Eqs.(22) and (24), we can calculate that :

$$\begin{aligned} |\,F(s,z)\,|^2 = \sin^2\delta_0^2 + 9\left[(\mathrm{Re}\,z)^2 + (\mathrm{Im}\,z)^2\right]\sin^2\delta_1^1 + 6\sin\delta_0^2\ \sin\delta_1^1\Big[(\mathrm{Re}\,z)\cos\delta_0^2\ \cos\delta_1^1 \\ -(\mathrm{Im}\,z)\cos\delta_0^2\ \sin\delta_1^1 + (\mathrm{Im}\,z)\sin\delta_0^2\ \cos\delta_1^1 + (\mathrm{Re}\,z)\sin\delta_0^2\ \sin\delta_1^1\Big]. \end{aligned} \tag{37}$$

As previously, our interest lies in studying the Legendre zeros of the amplitude. Since they are also automatically minima of $|F(s,z)|$, they fulfill the relation :

$$\frac{\partial\ |F(s,z)|^2}{\partial\ \mathrm{Re}\, z} = 0\,. \tag{38}$$

Going back to the task at hand, we notice that Eq.(38) can lead to an expression of the phase shift $\delta_1^1(s)$:

$$\begin{aligned} \frac{\partial\ |F(s,z)|^2}{\partial\ \mathrm{Re}\, z} = 0 \;\Leftrightarrow\; & 3\,(\mathrm{Re}\, z)\, \sin^2\!\delta_1^1 \,+\, \sin\delta_0^2\ \sin\delta_1^1\ \cos\delta_0^2\ \cos\delta_1^1 \,+\, \sin^2\!\delta_0^2\ \sin^2\!\delta_1^1 \,=\, 0 \\ & \text{and } z = z_0(s)\,. \\ \Leftrightarrow\; & 3\,(\mathrm{Re}\, z_0(s))\, \tan\delta_1^1 \,+\, \sin^2\!\delta_0^2\,.\ \tan\delta_1^1 \;=\; -\frac{1}{2}\sin 2\,\delta_0^2\,. \end{aligned} \tag{39}$$

$$\Leftrightarrow\; \tan\delta_1^1 \;=\; \frac{-\frac{1}{2}\sin 2\,\delta_0^2}{3\,(\mathrm{Re}\, z_0(s)) \,+\, \sin^2\!\delta_0^2}\,. \tag{40}$$

Therefore, we see that the Legendre zeros also provides us with a unitarization procedure, because it enables us to determine $\delta_1^1(s)$, so that $f_1^1(s)$ is completely defined in Eq.(24). Actually, $\delta_1^1(s)$ depends on $\delta_0^2(s)$ in Eq.(38). However, that is not a problem, as A. Schenk parametrized the exotic S-wave phase shift in [13] for our energy range :

$$\tan\delta_0^2\,(s) \;=\; \sqrt{\frac{s-4\,M_\pi^2}{s}}\ \left[a_0^2 \,+\, \tilde{b}_0^2 \left(\frac{s-4\,M_\pi^2}{4\,M_\pi^2}\right) \,+\, c_0^2 \left(\frac{s-4\,M_\pi^2}{4\,M_\pi^2}\right)^2 \right] \left(\frac{4\,M_\pi^2 - s_0^2}{s-s_0^2}\right), \tag{41}$$

$$\begin{aligned} \text{where}\ \ \tilde{b}_0^2 \;&=\; b_0^2 \,-\, a_0^2\ \frac{4\,M_\pi^2}{s_0^2 \,-\, 4\,M_\pi^2} \,+\, (a_0^2)^3, \\ a_0^2 \;&=\; -\,0.042\,, \\ b_0^2 \;&=\; -\,0.075\,, \\ c_0^2 \;&=\; 0\,, \\ s_0^2 \;&=\; -\,(685)^2\ \mathrm{MeV}. \end{aligned} \tag{42}$$

Moreover, as Eq.(27) showed, $|\sin\,\delta_0^2| \ll 1$. Hence, we see on Eq.(40) that when :

$$\mathrm{Re}\,[z_0(s)] \;\longrightarrow\; 0 \qquad \Leftrightarrow \qquad s \;\longrightarrow\; M_\rho^2 \qquad (\text{cf. Eq.(29)})\,, \tag{43}$$

$$\text{then,}\qquad \tan\delta_1^1(s) \;\longrightarrow\; \infty \qquad \Leftrightarrow \qquad \delta_1^1(s) \;\longrightarrow\; \frac{\pi}{2} \,+\, n\,\pi\,, \quad \mathrm{n}\;\in\;\mathbb{Z}\,. \tag{44}$$

We plotted the graph of $\delta_1^1(s)$ of Eq.(40) as a function of $\sqrt{s}$ using two different methods to look for the zero contour $\mathrm{Re}\, z_0(s)$.

Method A : We calculated the isospin amplitudes $F^1(s,z)$ and $F^2(s,z)$ using Eq.(18.1) of [4] and Eq.(31) for the expression of the function $A(t,s,u)$:

$$F^1(s,t) = A(t,s,u) - A(u,s,t)\,, \qquad (45)$$
$$F^2(s,t) = A(t,u,s) + A(u,s,t)\,.$$

As the $A(t,s,u)$ is symmetrical in its last two indices, the $F(s,z)$ in Eq.(20) is given by :

$$F(s,z) = A(t,s,u) \qquad (46)$$

Secondly, we used the inverse relation of Eq.(21) to calculate $f_1^1(s)$ and $f_0^2(s)$:

$$f_l^I(s) = \frac{1}{64\,\pi} \int_{-1}^{1} \mathrm{d}z \;\; P_l\,(z) \;\; F^I(s,z)\,, \qquad (47)$$

using *NIntegrate* on Mathematica to compute that integral numerically.

Then, we could calculate the function $z_0(s)$ using the formula obtained from Eq.(22) :

$$z_0\,(s) \; = \; - \; \frac{f_0^2(s)}{3\; f_1^1(s)}\;. \qquad (48)$$

Eventually, we plotted the graph of $\delta_1^1(s)$ using Eq.(48) for $z_0\,(s)$ and Eq.(41) for $\delta_0^2(s)$.

Method B : We calculated $z_0\,(s)$ simply by searching for the expression of z making $F(s,z)$ null. The Mathematica function we used is *FindRoot*.

One can see on Figures 1 and 2 the graphs of $\delta_1^1(s)$ obtained respectively with **Method A** and **Method B**. We added to the graphs three sets of experimental data for $\delta_1^1(s)$ taken from [14, 15, 16].

Moreover, the expression for $\delta_1^1(s)$ when it is obtained from $O(p^4)$ ChPT is the following [17] :

$$\delta_1^1(s) \; = \; \sigma(s)\,\mathrm{Re}\,f_1^1(s)\,, \qquad (49)$$

where the function $\sigma(s)$ is the same one as the $\sigma(x)$ defined for Eq.(31). We included the graph of this expression of $\delta_1^1(s)$ in Figures 1 and 2 so as to compare it with the plots obtained with the zeros method.

Observing the two figures, we notice a few things. Firstly, in the two plots, the results of the zeros method globally concur with the experimental data. That is another confirmation of the validity of the Legendre zeros method to study P-wave saturating vector resonances in the absence of a S-wave. In addition, we see that Method B gives better results than Method A, as they fit the experimental data more closely. That is understandable. Indeed, in that first method, we neglected the partial waves of order $l \geq 2$, whereas we did not neglect anything, albeit small, in Method B.

We also see that, as expected, the result for the $\delta_1^1(s)$ from $O(p^4)$ ChPT is not valid at energies of the order of the mass of the $\rho(770)$ or beyond. It does however naturally seem correct at energies below 500 MeV, as it coincides there with the zeros method result which is here phenomenologically confirmed.

We notice that the graph of $\delta_1^1(s)$ from the zeros method (we will take here the one from Method B as it is the best one) passes through $\frac{\pi}{2}$. From Eq.(44), we know that the value of s for which $\delta_1^1(s) = \frac{\pi}{2}$ is $s = M_\rho^2$. We can thus read on the graph the value of the resonance mass. We find $M_\rho = 0.77$ GeV, which is consistent with both the expected value and the value previously found for M_ρ in this work.

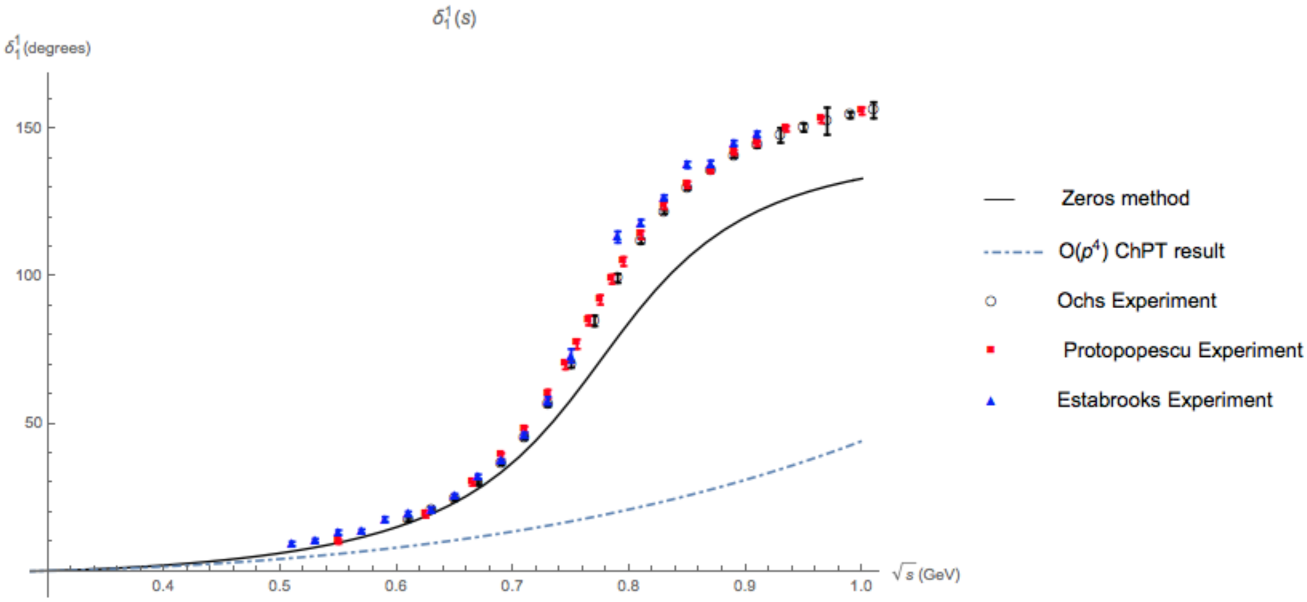

Figure 1. $\delta_1^1(s)$ obtained with Method A, experimental $\delta_1^1(s)$ [14, 15, 16] and $O(p^4)$ ChPT for $\delta_1^1(s)$ are also plotted.

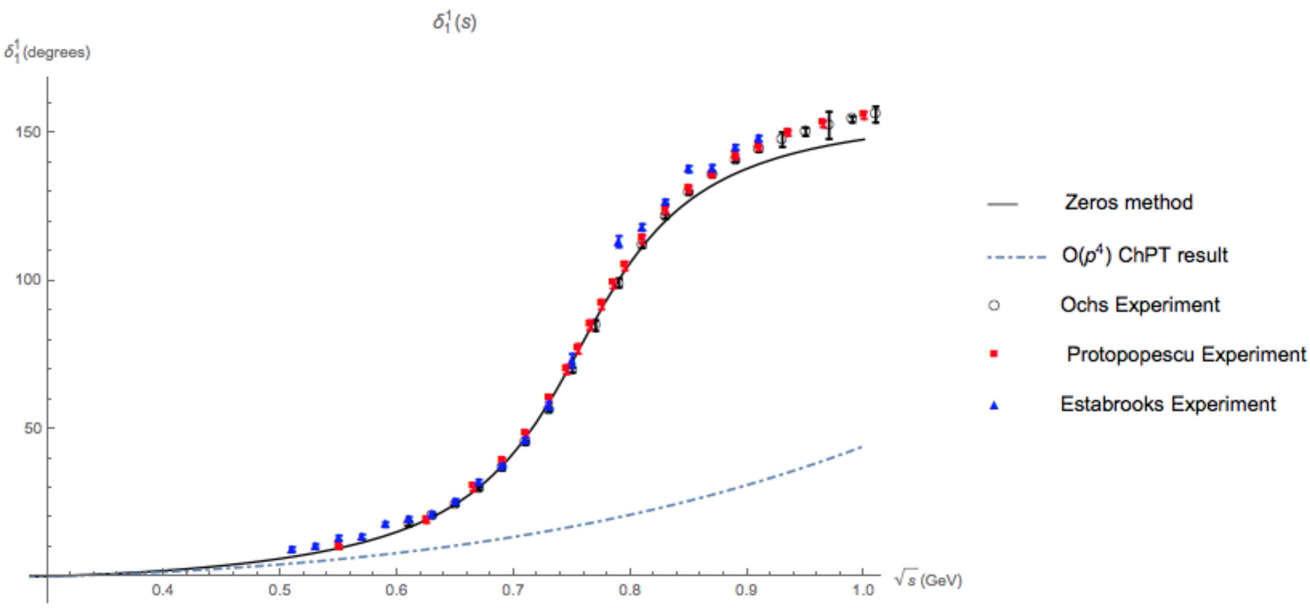

Figure 2. $\delta_1^1(s)$ obtained with Method B, experimental $\delta_1^1(s)$ [14, 15, 16] and $O(p^4)$ ChPT for $\delta_1^1(s)$ are also plotted.

2.3 Changes at $O(p^6)$

We can also comment on the changes that were reported when working at $O(p^6)$, the next order. Article [18] studied the subject in the case of the $\pi^-\pi^0 \to \pi^-\pi^0$ scattering, and we will give a brief review of their findings.

Firstly, [19] computed the $O(p^6)$ amplitude of that process, which was written in terms of the low-energy couplings $r_i(\mu),\ i = 1,..,6$. These couplings were assumed to be saturated by vector resonances, so $r_i(\mu) \sim r_i^V$, and were calculated and measured in [19] (similarly to how we explained the $l_i^r(\mu)$ were obtained in section 2.2.3).

The zero contour was drawn in [18] as a band, so it would contain the contours for values of μ comprised in $\mu \in [0.6,\, 0.9]$ GeV, since we know that the vector resonance contribution saturates the l_i^r and the r_i for a $\mu \simeq M_\rho$. At $O(p^4)$, the contour-band gave (with the help of Eq.(29)) $M_R \in [0.69,\, 0.91]$ GeV. At $O(p^6)$, the depth of the interval, linked to the uncertainty about the value of μ, was almost divided by four : the result was $M_R \in [0.80,\, 0.86]$ GeV. We see thus that apart from reducing the interval, adding the order 6 to the study does not modify our results a great deal.

We can however notice that the possible values for M_R at $O(p^6)$ do not include 0.77 GeV, which is the value we know it to be. As it was noticed in [18], if we were to change the sign of r_4^V, the interval for the resonance mass would transform into $M_R \in [0.78,\, 0.82]$ GeV, which brings us closer to the expected value. Updating the calculation of the constant in order to verify it might thus be an interesting approach before carrying out more calculation at this order.

From the results that we have introduced here, we can see that the order four already provides us with an accurate estimate of the zeros and the resonance mass, and that these are not modified exceedingly by the next order.

2.4 Conclusion

As a conclusion for this section 2, we can say that the Legendre zeros method is successful in :

- finding the resonance mass knowing the phenomenological values of the coupling constants,
- providing a unitarization procedure,

from a scattering amplitude given by Chiral Perturbation Theory, for a P-wave saturating vector resonance and in the absence of a S-wave. This was not trivial since, as we explained, the validity range of ChPT ends considerably below the mass of the vector resonance. Using the smoothness of the zero contour of the amplitude however, we succeeded in obtaining the correct results. It seems thus that the contour manages to retrieve from the chiral amplitude the information relevant at $E \simeq M_\rho$, which is enclosed in the coupling constants of the effective theory.

We used our knowledge of the $\pi^-\pi^0 \to \pi^-\pi^0$ process and of the existence of the ρ-resonance several times, while applying the zeros method in this section. Indeed, we knew that the $\rho(770)$ intervened in the process and that it was the only vector resonance involved at such energies. That justified the fact that it saturated the P-wave around $E \simeq M_\rho$ in Eq.(23). Moreover, we knew that the S-wave did not represent any particle, and that it was therefore a tenuous contribution to the amplitude, as we said so to obtain Eq.(27). We also used our phenomenological knowledge of $\overline{l_1}$ and $\overline{l_2}$ to compute the resonance mass and find the graphs in sections 2.2.3 and 2.2.4. Finally, knowing what we should obtain, we were able to confirm the accuracy of the method.

In the following section, we will apply the same method to the scattering of $W_L Z_L \to W_L Z_L$. This is a process that has a dynamics similar to the one of $\pi^- \pi^0 \to \pi^- \pi^0$, but that cannot yet be recreated experimentally, so we know very little about it. We thus hope that this Legendre zeros method will give us some new information concerning it. Additionally, as we cannot set this process up experimentally, the coupling constants of the corresponding effective theory are unknown to us, so every result obtained will be a function of them.

3 Electroweak case : Study of $W_L Z_L \to W_L Z_L$

3.1 The equivalence theorem

There is a relation between the Goldstone bosons π^a, that give mass to the gauge bosons $W^{\pm}$ and Z, and their longitudinal components, the $W_L^{\pm}$ and Z_L. The equivalence theorem gives us the link between their scattering amplitudes [2, 20] :

$$A\left(V_L^a V_L^b \to V_L^c V_L^d\right) = A\left(\pi^a \pi^b \to \pi^c \pi^d\right) + O\left(\frac{M_V}{E}\right). \tag{50}$$

where M_V is the mass of the gauge bosons and V_L^a are the longitudinally polarized gauge bosons. a, b, c and d are the isospin or electric charge indices.

With the help of an electroweak theory implementing the spontaneous gauge symmetry breaking, we can thus calculate our scattering amplitude $A\left(W_L Z_L \to W_L Z_L\right)$. As we will see in section 3.2, we will consider an effective theory of that electroweak one, and its validity range will be confined to energies $E \ll \Lambda_{EW} = 4\pi v$. However, the $O\left(\frac{M_V}{E}\right)$ in the previous theorem (50) indicates that it is only valid at high energies $E \gg M_V$, whereas our effective electroweak theory only works at low ones. In order to be able to use the relation between the Goldstone bosons and the gauge bosons scattering amplitudes depicted in the previous theorem with our effective electroweak theory, we have to restrict it somewhat [21] :

$$A^{(4)}\left(V_L^a V_L^b \to V_L^c V_L^d\right) = A^{(4)}\left(\pi^a \pi^b \to \pi^c \pi^d\right) + O\left(\frac{M_V}{E}\right) + O(g, g') + O\left(\frac{E^5}{\Lambda_{EW}^5}\right), \tag{51}$$

where $A^{(4)}(V_L^a V_L^b \to V_L^c V_L^d)$ is the gauge bosons scattering amplitude at $O(p^4)$, and $A^{(4)}(\pi^a \pi^b \to \pi^c \pi^d)$ is the Goldstone bosons scattering amplitude at $O(p^4)$ and at $O(g^0, g'^0)$.

3.2 The electroweak chiral lagrangian

There exists an alternative to the Higgs mechanism and the corresponding SM lagrangian $L_{\text{Higgs}} = (D_\mu \Phi)^\dagger (D^\mu \Phi) - V(\Phi)$, with the covariant derivative D_μ introducing the electroweak gauge bosons using the fields W_μ^k and B_μ. It has to reproduce the physics of the Higgs, since we know that the Higgs model is successful in explaining experiments, and it must be a strong interacting sector so it reproduces that physics using bound states. The non-linear sigma model provides us with that alternative. We will not go into much detail about it here, but the main points are the following.

Firstly, it implements the spontaneous symmetry breaking $SU(2)_L \otimes U(1)_Y \to U(1)_{em}$. Therefore, as three generators are broken here, three Goldstone bosons π^a , $a = 1, 2, 3$ are created. The lagrangian can be rewritten so as to make mass terms for the gauge bosons appear and the Goldstone bosons disappear. Actually, the π^a do not exactly vanish. They are absorbed into the gauge bosons which, as they become massive, gain a longitudinal component. The three Goldstone bosons effectively represent the degrees of freedom of these three new longitudinal components $W_L^{\pm}$ and Z_L. In this model, the Goldstone bosons are parametrized as such :

$$U(x) = \exp\left[\frac{i}{v}\,\pi^a\,\tau^a\right] = \exp\left[i\frac{\sqrt{2}}{v}\Phi\right], \quad \text{where} \quad \Phi(x) = \begin{pmatrix} \frac{\pi^0}{\sqrt{2}} & \pi^+ \\ \pi^- & -\frac{\pi^0}{\sqrt{2}} \end{pmatrix} \tag{52}$$

and π^a are the Goldstone bosons eigenstates in the isospin basis,

$\pi^{\pm}$ and π^0 are the Goldstone bosons eigenstates in the electric charge basis,

τ^a are the Pauli matrices,

$v = \dfrac{1}{\sqrt{\sqrt{2}\,G_F}} \simeq 246$ GeV is the vacuum expectation value of the Higgs in the Higgs mechanism.

U transforms under the gauge group $SU(2)_L \otimes U(1)_Y$ in the following way :

$$U \longrightarrow L\,U\,R^{\dagger}\ , \quad \text{where } L \in SU(2)_L \text{ and } R \in U(1)_Y. \tag{53}$$

Moreover, there is an equivalence between these symmetries and SSB :

$$SU(2)_L \otimes U(1)_Y \to U(1)_{em} \quad \Leftrightarrow \quad SU(2)_L \otimes SU(2)_R \to SU(2)_{L+R}\,. \tag{54}$$

Therefore, we will use whichever one of the two is more convenient in order to develop our effective field theory.

Furthermore, it has been proven that the relation $M_W = M_Z \cos\theta_W$ and the smallness of the oblique T parameter are theoretically linked to the custodial symmetry $SU(2)_{L+R}$. These relations concur with the phenomenology to a high degree of precision, so we want to keep the custodial symmetry intact to represent them. However, the $U(1)_Y$ interactions (of coupling constant g') explicitly break the $SU(2)_L \otimes SU(2)_R$ and more alarmingly the $SU(2)_{L+R}$ symmetries. We will thus work in the limit of $g' \to 0$ and conserve the custodial symmetry (and the chiral one), and keep both the relation between the gauge bosons masses and the smallness of the T.

Next, we want to build an effective field theory for the non-linear sigma model. The two fundamental blocks to create it are the degrees of freedom at low energies and the symmetries it has to conserve. The three Goldstone bosons π^a and the gauge bosons enclosed in the covariant derivative are the only degrees of freedom at energies of the order of 1 TeV. Indeed, even though we choose the chiral symmetry over the gauge one in Eq.(54), the D_μ has to contain W_μ^k and B_μ since these represent the gauge bosons which we know exist. We say that $SU(2)_L \otimes U(1)_Y$ is *gauged*. Moreover, as we said, our electroweak sigma non-linear model is invariant under gauge symmetry, so it is too under the chiral one (cf. Eq.(54)), and it has to conserve CP. (We will not implement any CP-violation here, as it is not the point of the study to investigate that, and it would complicate unnecessarily the problem.) We see thus that we have the same starting blocks as we had for Chiral Perturbation Theory in section 2.1.2.2. Therefore, our effective electroweak theory will be very similar to the ChPT one, with :

- The Goldstone bosons taking the place of the pions
- A change of the scale : $f_\pi \longrightarrow v$ (The formulas for U in ChPT (Eq.(5)) and in this EW effective theory (Eq.(52)) give us the analogy.)

Sensibly, this theory will be called the Effective Chiral Electroweak Theory (EChET).

The most general effective lagrangian in the limit $g' \to 0$ at order $O(p^4)$ has the following expression [22, 23, 24] :

$$L_{\mathrm{EChET}} = \frac{v^2}{4} \langle (D_\mu U)^\dagger (D^\mu U) \rangle + \sum_{i=3,4,5} a_i \, O_i \,, \tag{55}$$

$$\begin{aligned}
\text{where} \quad & O_3 = i\, g \, \langle W_{\mu\nu} \, [V^\mu, V^\nu] \rangle, \\
& O_4 = \langle V_\mu \, V_\nu \rangle^2, \\
& O_5 = \langle V_\mu \, V^\mu \rangle^2, \\
& D_\mu U = \partial_\mu U + \frac{i}{2} \, g \, \tau^k \, W_\mu^k \, U - \frac{i}{2} \, g' \, \tau^3 \, U \, B_\mu \,, \\
& V_\mu = (D_\mu U) \, U^\dagger, \\
& W_{\mu\nu} = \frac{1}{2} \, \tau^k \, W_{\mu\nu}^k \,, \\
& W_{\mu\nu}^k \text{ and } B_{\mu\nu} \text{ being the gauge field strength tensors.}
\end{aligned} \tag{56}$$

There are also eight other order four operators O_i that do not conserve the custodial symmetry $SU(2)_{L+R}$ in the limit $g' \to 0$ [8]. We will not consider them in this work.

The $O(p^2)$ term of the lagrangian (55) (the first term) provides us with a mass term for the gauge bosons. Since this kinetic term has to be properly normalized, its constant is fixed to $\frac{v^2}{4}$. We see here again the analogy between Chiral Perturbation Theory and this Effective Chiral Electroweak Theory : in Eq.(11) in the ChPT case, the kinetic constant was $\frac{f_\pi^2}{4}$. This concurs with the $f_\pi \longleftrightarrow v$ analogy we made in the list before Eq.(55) using the parametrizations of the U.

In addition, the O_i operators in Eq.(55) are of order four. The a_i are their coupling constants, similarly to the l_i in ChPT with two flavours. The coupling constants contain the information on the heavier degrees of freedom that have been integrated out from the action in order to create the effective theory. By analogy with ChPT (cf. section 2.1.4), we know that the EChET scale Λ_{EW} has this expression :

$$\Lambda_{ChPT} = 4\pi f_\pi \simeq 1.2 \text{ GeV} \qquad \text{so} \qquad \Lambda_{EW} = 4\pi v \simeq 3 \text{ TeV}. \tag{57}$$

As we explained in section 2.1.2.2 in the case of ChPT, it was interesting for us to organize the lagrangian (55) in terms with an increasing number of covariant derivatives D_μ : since ∂_μ is similar to p_μ and we are working at low energies, it enables us to make perturbative calculations. This organization entails a perturbative expansion of the theory in powers of $\frac{p^2}{\Lambda_{EW}^2}$ and $\frac{M_V^2}{\Lambda_{EW}^2}$, where M_V is the mass of the gauge bosons.

Furthermore, as we know that the Higgs boson exists, we want to include it in our theory. We can do so by multiplying every term of the lagrangian (55) by $f_i(H)$, an arbitrary polynomial of the Higgs field H. It thus transforms the EChET lagrangian (55) into :

$$L_{\mathrm{EChET}} = \frac{v^2}{4} \langle (D_\mu U)^\dagger (D^\mu U) \rangle \, f_0(H) + a_4 \, \langle V_\mu \, V_\nu \rangle^2 \, f_4(H) + a_5 \, \langle V_\mu \, V^\mu \rangle^2 \, f_5(H) \,, \tag{58}$$

where $f_i(0) = 1$. We take $f_0(H) = 1 + \frac{2H}{v}$ so that the $O(p^2)$ term of Eq.(58) gives us the same interaction between the Higgs and the Goldstone bosons as would $L_{\text{SM, Higgs}}$. We also choose $f_4(H) = 1$ and $f_5(H) = 1$ because the interactional Higgs in this operator does not contribute to the process we are considering. (The interaction with it would be between at least 4 Goldstone bosons and one Higgs so it would not intervene in the scattering studied.)

We omitted the O_3 operator of the lagrangian (55) in the new (58) one because as we said, we are considering this effective electroweak theory in order to ultimately calculate the amplitude $A\,(W_L Z_L \;\to\; W_L Z_L)$ via the restricted equivalence theorem (51). Indeed, said theorem implies working at $O(g^0,\, g'^0)$, and in this $g \longrightarrow 0$ limit, the O_3 operator vanishes.

Moreover, we notice that at $O(g^0,\, g'^0)$, the masses of the gauge bosons are null : $M_W = M_Z = 0$. Indeed, when working in these limits, the covariant derivative D_μ becomes only ∂_μ (cf. Eqs.(56)). Hence, there will be no W_μ^k nor B_μ fields in the order two term of lagrangian (58) to create mass terms for the gauge bosons. These are thus massless in this limit. That is why we will have to work in the $M_{V^a} \to 0$ limit while computing the scattering amplitude $A^{(4)}(\pi^a\,\pi^b \;\to\; \pi^c\,\pi^d)$.

There are no mass terms for the π^a in lagrangian (58). We will proceed by analogy with the ChPT case to explain so. In the chiral theory, the Goldstone bosons were given mass by the last two terms of lagrangian (11) and the $s = M$ mass matrix of the quarks, as we explained in Eq.(15). In the electroweak case, there are no such terms in lagrangian (58), and there is no mass matrix either, which shows us that the Goldstone bosons are massless here : $M_{\pi^a} = 0$. In addition, the equivalence theorem gives the scattering amplitude analogy :

$$\text{" } \pi^a = V_L^a \text{ "}, \quad \text{which entails} \;\; M_{\pi^a} = M_{V^a}\,. \tag{59}$$

Thus, since $M_{\pi^a} = 0$, it is consistent with (59) that the equivalence theorem has us working at $O(g^0,\, g'^0)$ (where the gauge boson masses M_{V^a} are null).

Additionally, the last terms of Eq.(51) imply that our calculation will only be valid at energies comprised between $M_V \ll E \ll \Lambda_{EW} = 4\pi v$. First, we saw on Figures 1 and 2 that the $O(p^4)$ ChPT result was valid only up until $E \simeq 500$ MeV $\simeq 2\pi f_\pi$. By analogy, we conclude that our Effective Chiral Electroweak Theory will accurately describe reality only for energies $E \leq 2\pi v \simeq 1.5$ TeV. Furthermore, we know that when we use the zero contour, the validity range increases considerably. In ChPT, we saw on Figure 2 that the zero contour result was valid at least until $E \simeq 800$ MeV, as it matched the experimental data well at this energy. Therefore, we can expect our electroweak results obtained with the zeros method to be valid at least until $E \simeq 2$ TeV.

On the whole, at $E \ll \Lambda_{EW}$, the electroweak effective theory represents the SM with or without Higgs. At $E \gg \Lambda_{EW}$, the Effective Electroweak Chiral Theory is not valid anymore, even while using the smoothness of the zero contour. Thus, it cannot enable us to accurately find any resonance at these energies. We see that the study we will carry out will show us the vector resonances that are involved in our scattering process at energies of the order of 1 TeV.

3.3 The scattering amplitude $A^{(4)}(W_L Z_L \;\to\; W_L Z_L)$

As we said, the equivalence theorem relates $A^{(4)}(W_L Z_L \to W_L Z_L)$ to the corresponding Goldstone bosons scattering amplitude $A^{(4)}(\pi^-\pi^0 \;\to\; \pi^-\pi^0)$. $A^{(4)}(\pi^-\pi^0 \;\to\; \pi^-\pi^0)$ can be calculated using lagrangian (58). Moreover, this L_{EChET} can be decomposed into two parts :

$$L_{\text{EChET}} = L_{\text{EChET, Higgsless}} + L_{\text{EChET, Higgs}}\,, \tag{60}$$

$$\text{where}\quad L_{\text{EChET, Higgsless}} = \frac{v^2}{4}\,\langle (D_\mu U)^\dagger\,(D^\mu U)\rangle \,+\, a_4\,\langle V_\mu V_\nu\rangle^2 \,+\, a_5\,\langle V_\mu V^\mu\rangle^2\,,$$
$$L_{\text{EChET, Higgs}} = \frac{v^2}{4}\,\langle (D_\mu U)^\dagger\,(D^\mu U)\rangle\,\frac{2H}{v}\,. \qquad (61)$$

Actually, we can notice that $L_{\text{EChET, Higgsless}}$ is identical to L_{ChPT} at $O(p^4)$ with two flavours (as the two effective theories were obtained with the same starting elements), with two differences : the pions were replaced by the Goldstone bosons, and the constants $(f_\pi,\,\overline{l_1},\,\overline{l_2})$ by $(v,\,\overline{a}_5,\,\overline{a}_4)$. Consequently, the Higgsless contribution to the $A^{(4)}(\pi^-\pi^0 \to \pi^-\pi^0)$ required by the equivalence theorem (51) has the form of $A\,(t,s,u)$ from Eq.(31), with the appropriate change of constants and, as we said in the previous section, calculated at $M_V \to 0$. This limit was calculated in [4] and gives :

$$A^{(4)}(\pi^-\pi^0 \to \pi^-\pi^0)_{\text{Higgsless}} \;=\; \frac{t}{v^2} + \frac{1}{96\,\pi^2\,v^4}\left[3\,t^2\,\ln\left(\frac{\mu_1^2}{-t}\right)\right.$$
$$\left. +\; s(s-u)\,\ln\left(\frac{\mu_2^2}{-s}\right) + \,u(u-s)\,\ln\left(\frac{\mu_2^2}{-u}\right)\right], \qquad (62)$$

where the scales μ_1 and μ_2 are defined as :

$$\ln\frac{\mu_1^2}{M_V^2} \;=\; \frac{2}{3}\,\overline{a}_5 \,+\, \frac{1}{3}\,\overline{a}_4 \,+\, \frac{5}{6}\,,$$
$$\ln\,\frac{\mu_2^2}{M_V^2} \;=\; \overline{a}_4 \,+\, \frac{7}{6}\,. \qquad (63)$$

and as we are working in the $M_V \to 0$ limit,

$$u \,=\, -s-t \qquad \text{and} \qquad t \,=\, \frac{s}{2}\,(z-1)\,. \qquad (64)$$

The two logarithms are the only functions that will keep a dependance in $M_V \neq 0$, so as for infinities in the amplitude to be avoided. We will take for M_V the isospin vector mass $M_V = \frac{2M_W+M_Z}{3} \simeq 84$ GeV.

Moreover, we define the renormalized coupling constants in the following way in the $\overline{\text{MS}}$-scheme :

$$a_4^r(\mu) = \frac{1}{4}\,\frac{1}{48\,\pi^2}\left(\overline{a}_4 \,-\, 1 \,+\, \ln\frac{M_V^2}{\mu^2}\right),$$
$$a_5^r(\mu) = \frac{1}{4}\,\frac{1}{96\,\pi^2}\left(\overline{a}_5 \,-\, 1 \,+\, \ln\frac{M_V^2}{\mu^2}\right). \qquad (65)$$

We took this definition to be the same as in [25, 26]. This is why it results different from the l_i^r one in (33). We can also notice that the M_V-dependence in (62) is caused by the fact that $A^{(4)}(\pi^-\pi^0 \to \pi^-\pi^0)_{\text{Higgsless}}$ is expressed in terms of $\overline{a}_4$ and $\overline{a}_5$, and we see in Eq.(65) that changing from variables $(a_4^r(\mu)\,,\,a_5^r(\mu))$ to $(\overline{a}_4\,,\,\overline{a}_5)$ introduces indeed M_V. The natural values of the coupling constants are $\overline{a}_{4,\,5} \sim O(1)$.

In order to have the full Goldstone bosons scattering amplitude, the contribution from $L_{\text{EChET, Higgs}}$ has to be added. In the $M_V \to 0$ limit, the covariant derivative D_μ is just ∂_μ. Therefore,

$$\begin{aligned} L_{\text{EChET, Higgs}} &= \frac{v^2}{4} \; \frac{2H}{v} \; \langle (\partial_\mu U)^\dagger \, (\partial^\mu U) \rangle \text{ , where the expression of } U \text{ can be found in Eq.(52),} \\ &= \frac{v}{2} \; H(x) \; \frac{2}{v^2} \; \langle \partial_\mu \begin{pmatrix} \frac{\pi^0}{\sqrt{2}} & \pi^+ \\ \pi^- & -\frac{\pi^0}{\sqrt{2}} \end{pmatrix} \, \partial^\mu \begin{pmatrix} \frac{\pi^0}{\sqrt{2}} & \pi^+ \\ \pi^- & -\frac{\pi^0}{\sqrt{2}} \end{pmatrix} \rangle \text{ developing the exp in Eq.(52),} \\ &= \frac{1}{v} \; H \; \Big[\, (\partial_\mu \pi^0) \, (\partial^\mu \pi^0) \, + \, 2 \, (\partial_\mu \pi^+) \, (\partial^\mu \pi^-) \, \Big] \text{ calculating the trace,} \end{aligned} \tag{66}$$

where H and the π^a are the bosons fields.

So,

$$A^{(4)}(\pi^-\pi^0 \to \pi^-\pi^0)_{\text{Higgs}} \;=\; - \; \frac{t^2}{v^2} \; \frac{1}{t \, - \, M_H^2} \; , \tag{67}$$

where $M_H \simeq 125$ GeV. Here, we only consider the leading tree level Higgs contribution and are not doing a full calculation at $O(p^4)$.

We now know every part of :

$$\begin{aligned} A^{(4)}(\pi^-\pi^0 \to \pi^-\pi^0) \; &= \; A^{(4)}(\pi^-\pi^0 \to \pi^-\pi^0)_{\text{Higgsless}} \; + \; A^{(4)}(\pi^-\pi^0 \to \pi^-\pi^0)_{\text{Higgs}} \\ &\simeq \; A^{(4)}(W_L Z_L \to W_L Z_L). \end{aligned} \tag{68}$$

3.4 Legendre zeros method applied to $W_L Z_L \to W_L Z_L$

3.4.1 Principles

Firstly, as we said, $L_{\text{EChET, Higgsless}}$ is identical to the ChPT lagrangian at $O(p^4)$ with two flavours, but for the pions that are replaced by Goldstone bosons, the kinetic constant f_π that we exchange for v and the order four coupling constants $(\bar{l}_1, \bar{l}_2)$ that become $(\bar{a}_5, \bar{a}_4)$. Therefore, one can expect to observe a dynamics for $W_L Z_L \to W_L Z_L$ that is similar to the one of $\pi^-\pi^0 \to \pi^-\pi^0$, but only on one condition : the P-wave has to be saturated by a vector resonance at the resonance mass, leaving the S-wave to be a small additional contribution to the amplitude, just as in the chiral case. We will neglect the partial waves of $l \geq 2$ in this electroweak case as we had in the chiral one, and will assume that the LECs are saturated by the vector resonances. We will then be able to apply the same Legendre zeros method as we had in sections 2.2.2, 2.2.3, 2.2.4, and use the zeros of the scattering amplitude to deduce the position of the $I = 1$ vector resonance.

The method we apply in this electroweak case contains three steps.

- First, we search for the zeros of the function $A(s, z)$ - which is no other than the scattering amplitude $A^{(4)}(W_L Z_L \to W_L Z_L)$ written in terms of s and z using Eq.(64). This provides us with a relation between s and z (as it had in the chiral case), that we can express as : $z = z_0(s)$.

- Then, we look for the minimum resonance mass for each pair $(\bar{a}_4, \bar{a}_5)$. We do so by using equation (29), satisfied by P-wave saturating vector resonance masses. The minimal resonance mass is researched as opposed to the maximum one because we try to rule out regions where there are no resonances from below, as the experiments always proceed increasing the energy.

- Finally, we establish a condition designed to check whether the P-wave indeed dominates the amplitude around the resonance mass. In the cases where the condition is fulfilled, our use of Eq.(29) to find the mass is validated. In the other cases, it teaches us that there is no vector resonance there to saturate the P-wave. This is how we obtain our condition :

  Using the zeros of the amplitude, we obtain from Eq.(22) that :

$$f_0^2\,(s) \,+\, 3\; z_0\,(s)\; f_1^1\,(s) \;=\; 0\,. \tag{69}$$

  So at the resonance location, as $\mathrm{Re}\,(z_0(M_R^2)) = 0$ (cf. Eq.(29)) :

$$|\, z_0(M_R^2)\,| \;=\; |\,\mathrm{Im}\,(z_0(M_R^2))\,| \;=\; \left|\, \frac{f_0^2(M_R^2)}{3\; f_1^1(M_R^2)} \,\right|. \tag{70}$$

  As a result, calculating $|\, z_0(M_R^2)\,|$ enables us to have an accurate estimate of the S-wave to P-wave ratio at the resonance mass. The condition we impose for our zeros method to be applicable is :

$$|\, z_0(M_R^2)\,| \;=\; |\,\mathrm{Im}\,(z_0(M_R^2))\,| \;<\; \lambda\,. \tag{71}$$

  Then, we have to choose a value for λ so that the condition successfully manages to rule out the $(\bar{a}_4,\, \bar{a}_5)$ that do not really allow for a vector resonance. To start, in the pions case, we can compute $|\, z_0(M_\rho^2)\,| \;=\; 0.37$. Moreover, we judge that $\lambda = \frac{1}{2}$ is the maximum value of λ for which we can consider that the exiting partial waves satisfyingly fulfill : $|\, f_0^2(M_R^2)\,| \;\ll\; |\, f_1^1(M_R^2)\,|$. We will also consider $\lambda = \frac{1}{3}$ to see how the change in λ affects the results.

Furthermore, it can be noticed that Eqs.(22), (24) and (40) from the chiral case are still valid in EChET. Therefore, the amplitude zeros also provide $A(W_L Z_L \to W_L Z_L)$ with a unitarization procedure.

As we can also notice, the value that we take for λ has a direct impact on the convergence of the partial wave expansion of the amplitude. Indeed, as article [18] explained, in the $M_V \to 0$ limit, the partial wave expansion is convergent as $l \to \infty$ only when $z \in [-1,\, 1]$ (which is the physical region). Therefore, whenever $|\,\mathrm{Im}(z)\,| \neq 0$, it will not be convergent. In addition, as showed in [18], the larger $|\,\mathrm{Im}(z_0(M_R^2))\,|$ is, the more $A(M_R^2,\, z_0(M_R^2))$ will diverge as l increases. Thus, limiting $|\,\mathrm{Im}(z)\,|$ through λ also enables us to ensure a better convergence of the amplitude expansion.

3.4.2 Obtaining the graphs

First, as the scattering amplitude $A(s, z)$ is analytic, it fulfills the positivity conditions on the $\pi\pi \to \pi\pi$ scattering amplitude. These imply for $\bar{a}_4$ and $\bar{a}_5$ [10, 27] :

$$\bar{a}_5 \,+\, 2\,\bar{a}_4 \;\geq\; \frac{157}{40} \qquad \text{and} \qquad \bar{a}_4 \;\geq\; \frac{27}{20}\,. \tag{72}$$

Then, we can introduce the two graphs, Figures 3 and 4, that constitute the major results of this study. They display the minimum mass allowed for a vector resonance having a role in the $W_L Z_L$ elastic scattering, as a function of $\bar{a}_4$ and $\bar{a}_5$. Figure 3 is obtained not considering the Higgs contribution in Eq.(60). The second graph however, on Figure 4, takes the full L_{EChET} into account and is the valid solution of our study. We actually added the Higgsless plot in order to compare it with our Figure 4, and determine the influence that adding $L_{\mathrm{EChET,\, Higgs}}$ has on the full lagrangian

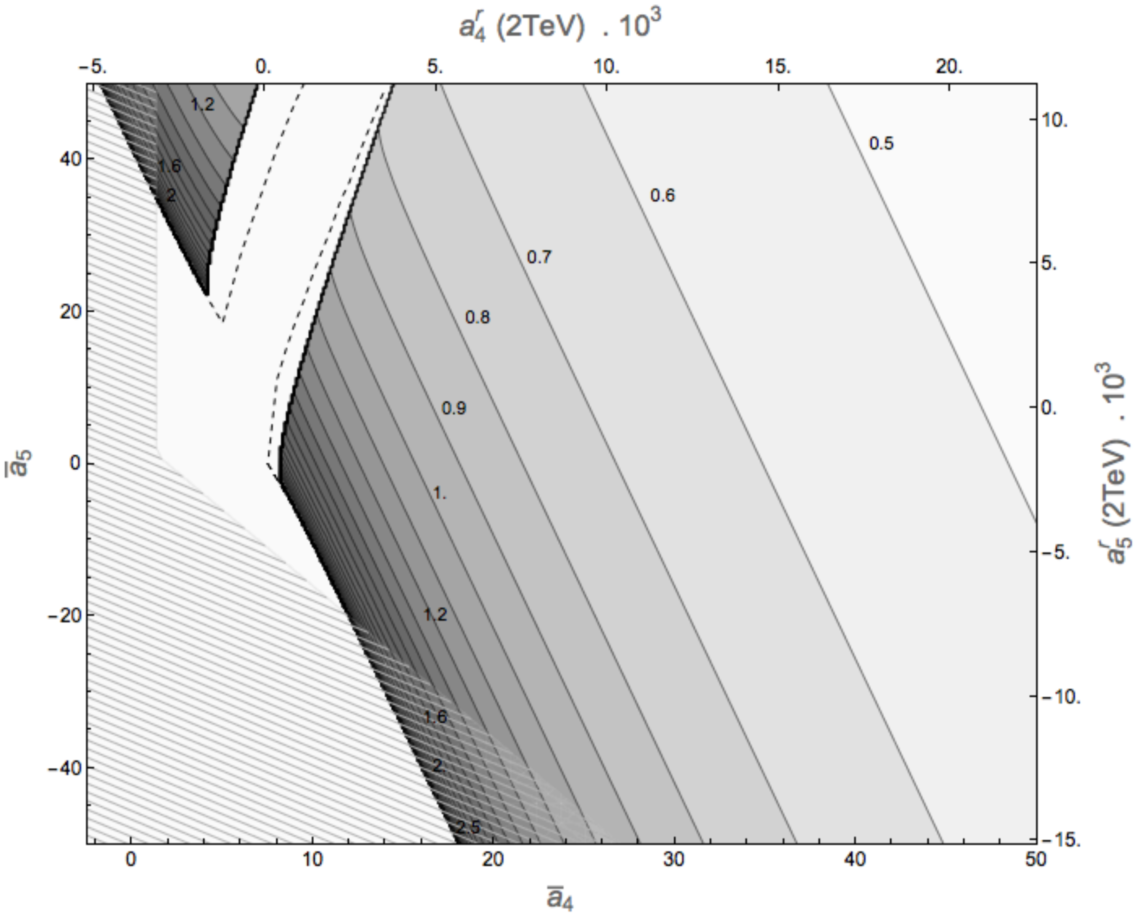

Figure 3. Resonance masses (in TeV) in the $(\overline{a}_4, \overline{a}_5)$ plane for $\lambda = \frac{1}{3}$ in a Higgsless world. Dashed line : change of contour if $\lambda = \frac{1}{2}$. Hatched zone : region of the $(\overline{a}_4, \overline{a}_5)$ plane forbidden by positivity conditions (cf. Eq.(72)).

L_{EChET}.

Also, as we said, we cannot recreate experimentally the $W_LZ_L \to W_LZ_L$ scattering, and it is why we do not know the values of $\overline{a}_4$ and $\overline{a}_5$. Hence, the resonance masses in Figures 3 and 4 are a function of these $O(p^4)$ coupling constants.

The graphs in Figures 3 and 4 should be understood in the following way. The shaded areas are the ones allowing for a vector resonance at energies $E \sim 1$ TeV. The contour lines separating the different shades indicate the $(\overline{a}_4, \overline{a}_5)$ pairs that share a same resonance mass belonging to a range of "significant" values that we chose. The white zones (whether they are below the hatched one or not) indicate both the regions for which no resonance mass M_R was found using the relation $\mathrm{Re}\,(z_0(M_R^2)) = 0$, and the ones for which the condition $|\,z_0(M_R^2)\,| < \lambda$ is not fulfilled. We considered $\lambda = \frac{1}{3}$, and added as a dashed line the general contour of the graph with $\lambda = \frac{1}{2}$. The hatched zone shows the $(\overline{a}_4, \overline{a}_5)$ that are forbidden by the positivity conditions in (72). Finally, we added to the graph the scales in terms of the renormalized coupling constants $a_4^r(\mu)$ and $a_5^r(\mu)$ with $\mu = 2$ TeV, using Eq.(65). We explain some of the programming that led to Figures 3 and 4 in the Appendix.

We also wondered about the cuts that we can see in Figure 4. They correspond to points that do not allow for any solution M_R to the equation $\mathrm{Re}\,(z_0(M_R^2)) = 0$. Article [18] managed to smooth them out, but the same method did not work in our case. We do not understand their existence.

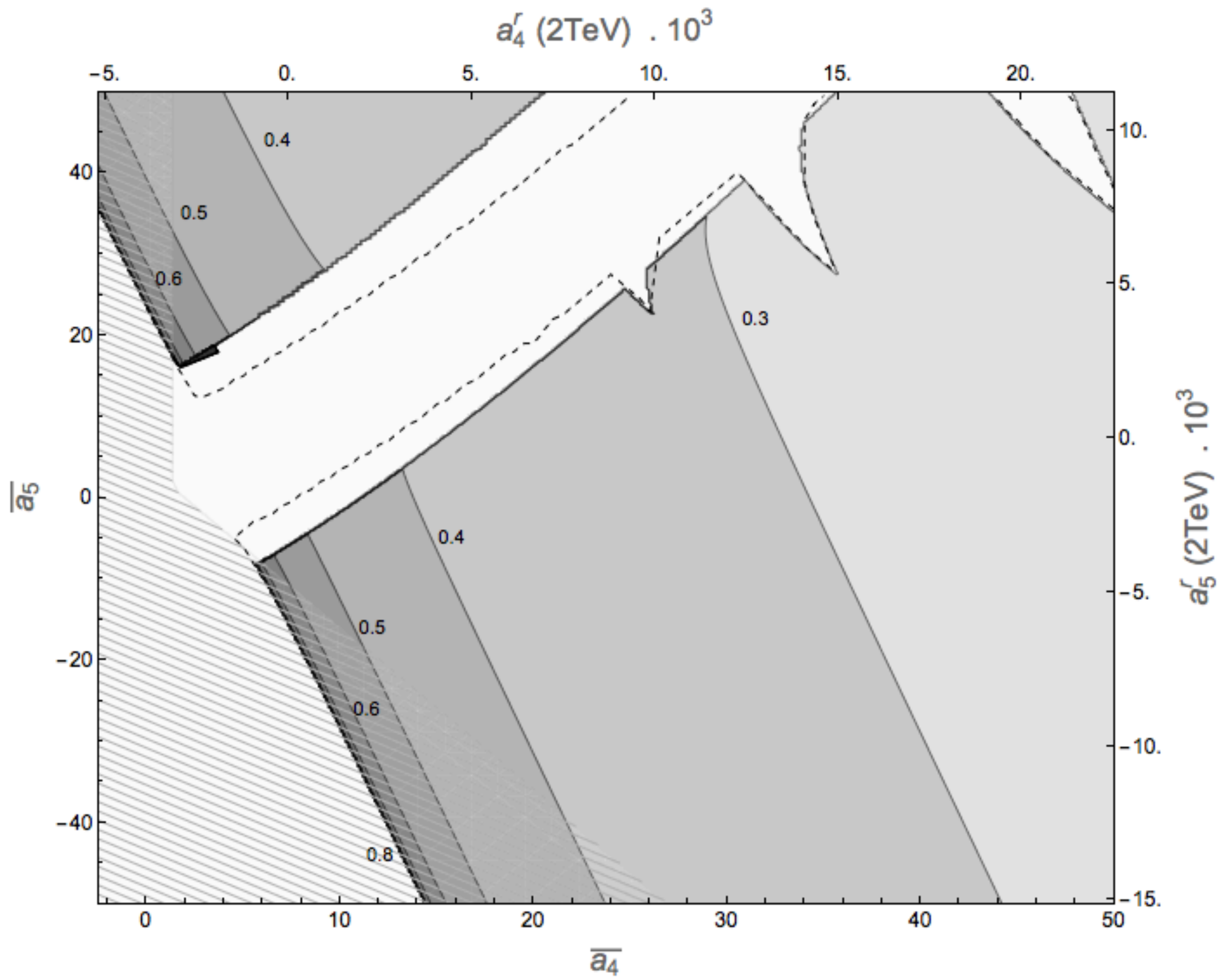

Figure 4. Resonance masses (in TeV) in the $(\overline{a}_4, \overline{a}_5)$ plane for $\lambda = \frac{1}{3}$, including the SM Higgs in the analysis (as done in Eqs.(67) and (68)). Dashed line : change of contour if $\lambda = \frac{1}{2}$. Hatched zone : region of the $(\overline{a}_4, \overline{a}_5)$ plane forbidden by positivity conditions (cf. Eq.(72)).

3.4.3 Results

Higgsless case : Firstly, we do not observe any resonance for $\overline{a}_4 \leq 8$ and $\overline{a}_5 \leq 22$ (with $\lambda = \frac{1}{3}$). The natural values for the coupling constants rule thus vector resonances out at energies $E \sim 1$ TeV.

Moreover, we can notice that although we displayed in Figure 3 resonance masses up to 2.5 TeV, our results in this study cannot be trusted above $E \simeq 2$ TeV, as we explained at the end of section 3.2. We also see that the $M_R \geq 1.6$ TeV only take each a small portion of the graph, and most of the portion they have is forbidden by the positivity conditions. Conversely, the resonance masses at the other end of the range ($M_R \leq 0.8$ TeV) occupy each a large area in the graph, and are not affected by the positivity constraints. They however only exist for suspiciously large values of the coupling constants $\overline{a}_{4,\,5}$, and we can wonder if such values really are plausible.

Case with the SM Higgs : To start with, we see that adding the Higgs contribution to the lagrangian has a large impact on the graph, in that this one differs quite considerably from the previous, Higgsless one. Moreover, most natural values of the coupling constants ($\overline{a}_4 \leq 5$ and $\overline{a}_5 \leq 16$ with $\lambda = \frac{1}{3}$) also exclude vector resonances. Additionally, all the masses we obtain are inferior to 0.8 TeV. However, the equivalence theorem on Eq.(51) specifically requires us to work at energies $E \gg M_V$, and $M_V \sim 0.1\,\mathrm{TeV}$. We will thus not consider the M_R comprised between 0.2 TeV and 0.5 TeV as trustworthy information. Therefore, our method proves (with its assumptions) that there are no vector resonances of mass $M_R \in [0.8,\, 2]$ TeV involved in the elastic scattering of $W_L Z_L$. Furthermore, it shows that only a very small part of the $(\overline{a}_4,\, \overline{a}_5)$ plane allows for a vector resonance of mass $M_R \in [0.5,\, 0.8]$ TeV, as most of the initial area allocated to those masses is excluded by the positivity conditions.

Finally, we see with the dashed contour on both Figures 3 and 4 which part of the $(\overline{a}_4,\, \overline{a}_5)$ plane was excluded by taking $\lambda = \frac{1}{3}$ instead of $\frac{1}{2}$. The line shows us in which measure would the graph change if we were to reduce λ some more. Indeed, some global contours of the graph seem completely independent of the value taken for λ. It is because they separate regions which have a solution M_R to the equation $\mathrm{Re}\,(z_0(M_R^2)) = 0$, from regions which do not, whatever λ be. However, we do consider $\frac{1}{3}$ to be an accurate value for λ, because it limits $\left| \frac{f_0^2(M_R^2)}{3\, f_1^1(M_R^2)} \right|$ satisfyingly, and it is close to the value that the ratio has in Chiral Perturbation Theory.

3.4.4 Comparison with other techniques and the experimental results

There are other methods that set out to determine the possible vector resonance masses as a function of the coupling constants. We will review some of their findings and compare them with our own results.

The Inverse Amplitude Method (IAM) is one of these methods. It uses the Padé approximants on the partial waves, and searches for poles of the denominator as indicators of resonances. It is developed in terms of coupling constants that are, but for small corrections, our a_4^r and a_r^5. A recent publication on the topic [28] reports masses in the following range : $M_R \in [1.5,\, 2.5]$ TeV, for coupling constants $a_{4,\,5}^r \in [-1,\, 1]\,.10^{-3}$ TeV, which approximately correspond to these values of $\overline{a}_4$ and $\overline{a}_5$: $\overline{a}_4 \in [5, 10]$ and $\overline{a}_5 \in [0, 10]$. We can see that the IAM results are not compatible with our own : they find some resonance masses in a range that our study ruled out : $M_R \in [1.5,\, 2]$ TeV. Moreover, the values of $\overline{a}_4$ and $\overline{a}_5$ they find do not, in our study, allow for vector resonances. We could not understand the origin of these discrepancies.

Additionally, a Resonance Chiral Electroweak Theory can also provide us with bounds on the minimum allowed mass for a vector resonance. A recent publication in the matter [29] studied the S and T oblique parameters, and deduced through a phenomenological comparison that the mass for vector resonances at these energies very likely had to be such that $M_R > 1.5$ TeV. This is in agreement with our results.

Let us now compare our results for vector resonance masses, which exclude them in the range of $[0.8\text{ TeV}, 2\text{ TeV}]$, with the experimental data. First, article [25] reported that no deviation from the SM was observed at the LHC for $\overline{a}_4 \leq 35$ and $-38 < \overline{a}_5 < 45$, which is encouraging as to the validity of our study. Moreover, we looked into the most recent publications from the CMS and ATLAS experiments. The CMS results exclude resonances with masses below 1.59, 1.73 and 2 TeV for final states of respectively WW [30], WZ [30] and ZZ [31]. Similarly, the ATLAS experiment findings reported in [32] to rule out resonances below 3 and 4 TeV when analyzing as final states respectively ZZ and ZW. We see thus that these experimental results are compatible with the ones we obtained in this study.

4 Conclusions

To conclude, we have introduced a method to find the possible vector resonances at $E \sim 1$ TeV using EChET. The technique uses the smoothness of the zeros of scattering amplitudes. We also saw that it provides a unitarization procedure for the amplitude. In addition, the method works as well for resonances of higher spins. The calculation might just be more cumbersome.

We worked here in the $W_L Z_L \to W_L Z_L$ channel because it only allows for a (P-wave, $I = 1$) component and for a (S-wave, $I = 2$) one, if higher orders ($l \geq 2$) are neglected (which corresponds to assuming a vector resonance saturation of the involved coupling constants). Since the S-wave with isospin $I = 2$ offers a tiny contribution because there is no resonance contributing to that partial wave, the P-wave dominates the amplitude. That made the development of the technique considerably easier.

First, we applied the method to the $\pi^-\pi^0 \to \pi^-\pi^0$ scattering at $O(p^4)$ in Chiral Perturbation Theory, of which the coupling constants have been measured. This enabled us to verify that the method indeed finds the $\rho(770)$ resonance that we know is involved in this process. We concluded that our technique works satisfyingly well, and even provides us with a unitarization procedure for the amplitude. We also commented on the small changes that the $O(p^6)$ corrections bring to our results.

Then, we applied this Legendre zeros method to the scattering amplitude of $W_L Z_L \to W_L Z_L$ at chiral $O(p^4)$. For the calculation of this amplitude, we used the equivalence theorem, which relates it to the corresponding Goldstone bosons scattering one. These Goldstone bosons were the ones to provide mass to the gauge bosons through the spontaneous chiral symmetry breaking. We could then work with the EChET lagrangian to calculate our amplitude. Using the zeros method, we explored the appropriate range of the $(\overline{a}_4, \overline{a}_5)$ plane and deduced the lightest resonance mass allowed for each of these points of the plane, assuming the saturation of the amplitude by the resonance. The result is shown on Figure 4, and excludes such resonances with masses $M_R \in [0.8, 2]$ TeV. The existence of vector resonances of masses $M_R \in [0.5, 0.8]$ TeV is permitted, but confined to a tiny part of the $(\overline{a}_4, \overline{a}_5)$ plane, as shown on the aforementioned graph.

To conclude, this Legendre zeros method gives results in the electroweak sector that are compatible with the latest experimental data.

This study could be carried on by investigating the reasons for the discrepancies between our results and the Inverse Amplitude Method findings. A similar study at order $O(p^6)$ could be undertaken as well, so as to add to the precision of our results. Finally, one could also use this technique to search for resonances of spin $J > 1$.

Acknowledgements

I wish to thank Jorge Portolés for his many explanations on the topic.

Appendix - Programming comments

These are the major points of the programming that led to Figures 3 and 4. Our Mathematica file is composed of three main functions.

The first one computes M_R for given $\overline{a}_4$ and $\overline{a}_5$, using *FindRoot* and the characteristic feature of the resonance mass :

$$\mathrm{Re}\left(z_0\left(M_R^2, \overline{a}_4, \overline{a}_5\right)\right) = 0. \tag{73}$$

Since the equivalence theorem requires us to work at energies $M_V \ll E \ll \Lambda_{EW}$, we ask of the program to look only for resonances in [0.2, 3] TeV. We noticed that we had to impose some limits for *FindRoot* to be able to compute the masses. Actually, we divided the mentionned interval into a hundred smaller ones and searched for a resonance mass in each of them, as it is possible that each $(\overline{a}_4, \overline{a}_5)$ pair allows for more than one resonance.

The second major function calculates a table that scans $\overline{a}_4 \in [-2.5, 50]$ and $\overline{a}_5 \in [-50, 50]$, and gives for each $(\overline{a}_4, \overline{a}_5)$ pair the possible masses calculated by the previous function.

The last function implements the condition (71) in our data. It keeps of the previous table, for each $(\overline{a}_4, \overline{a}_5)$, the minimum M_R that satifies (71). If no resonance could be found for these coupling constants, or if none survived condition (71), the function assigns $M_R = 0$ to the pair $(\overline{a}_4, \overline{a}_5)$.

Then, we could plot the graphs with *ListContourPlot* and using *RegionPlot* to hatch the area forbidden by the positivity conditions. Moreover, we noticed that the general contour of the graphs was very sensitive to the interval taken for the scan of the $\overline{a}_4$ and $\overline{a}_5$ ranges. Therefore, we took some additional points with a smaller interval in those regions. Part of the contour of the top section of Figure 4 seems slightly uneven compared to the rest of it. That is because we did not have time to compute all the additional points in that particular region.

In order to draw the dashed contours for $\lambda = \frac{1}{2}$, we selected the closest points to the shaded area that have a $M_R = 0$. We could trace the contour as a line with the Mathematica command *Graphics*[{ *Dashed, Line* [...] }].

References

[1] M. J. G. Veltman, *Acta Phys. Polon.* **B8** (1977) 475.

[2] B. W. Lee, C. Quigg, and H. B. Thacker, *Phys. Rev. Lett.* **38** (1977) 883–885.

[3] A. Pich, *Rept. Prog. Phys.* **58** (1995) 563–610.

[4] J. Gasser and H. Leutwyler, *Annals Phys.* **158** (1984) 142.

[5] G. Ecker, J. Gasser, A. Pich, and E. de Rafael, *Nucl. Phys.* **B321** (1989) 311–342.

[6] A. Martin and T. Spearman, "Elementary particle theory," North-Holland Pub. Co., Amsterdam, The Netherlands, 1970.

[7] B. R. Martin, D. Morgan, and G. Shaw, *Pion-pion interactions in particle physics*. 1976.

[8] A. Dobado, A. Gomez-Nicola, A. L. Maroto, and J. R. Pelaez, *Effective lagrangians for the standard model*. 1997.

[9] M. Pennington, *AIP Conf. Proc.* **13** (1973) 89.

[10] M. R. Pennington and J. Portoles, *Phys. Lett.* **B344** (1995) 399–406.

[11] A. Pich, I. Rosell, and J. J. Sanz-Cillero, *JHEP* **02** (2011) 109.

[12] D. G. Dumm, P. Roig, A. Pich, and J. Portoles, *Phys. Lett.* **B685** (2010) 158–164.

[13] A. Schenk, *Nucl. Phys.* **B363** (1991) 97–113.

[14] S. D. Protopopescu, M. Alston-Garnjost, A. Barbaro-Galtieri, S. M. Flatte, J. H. Friedman, T. A. Lasinski, G. R. Lynch, M. S. Rabin, and F. T. Solmitz, *Phys. Rev.* **D7** (1973) 1279.

[15] P. Estabrooks and A. D. Martin, *Nucl. Phys.* **B79** (1974) 301–316.

[16] W. Ochs, *Die Bestimmung von $\pi\pi$-Streuphasen auf Grundlage einer Amplitudenanalyse der Reaktion $\pi - p\pi - \pi + n$ bei 17 GeV/c Primärimpuls*. Phd, University of Munich, Munich, Germany, 1973.

[17] J. Gasser and U. G. Meissner, *Phys. Lett.* **B258** (1991) 219–224.

[18] A. Filipuzzi, J. Portoles, and P. Ruiz-Femenia, *JHEP* **08** (2012) 080.

[19] J. Bijnens, G. Colangelo, G. Ecker, J. Gasser, and M. E. Sainio, *Nucl. Phys.* **B508** (1997) 263–310. [Erratum : Nucl. Phys.B517,639(1998)].

[20] J. M. Cornwall, D. N. Levin, and G. Tiktopoulos, *Phys. Rev.* **D10** (1974) 1145. [Erratum : Phys. Rev. D11, 972 (1975)].

[21] A. Dobado and J. R. Peláez, *Nucl. Phys.* **B425** (1994) 110–136. [Erratum : Nucl. Phys. B434, 475 (1995)].

[22] A. C. Longhitano, *Phys. Rev.* **D22** (1980) 1166.

[23] A. C. Longhitano, *Nucl. Phys.* **B188** (1981) 118–154.

[24] T. Appelquist and G.-H. Wu, *Phys. Rev.* **D48** (1993) 3235–3241.

[25] O. J. P. Eboli, M. C. Gonzalez-Garcia, and J. K. Mizukoshi, *Phys. Rev.* **D74** (2006) 073005.

[26] M. Fabbrichesi and L. Vecchi, *Phys. Rev.* **D76** (2007) 056002.

[27] A. V. Manohar and V. Mateu, *Phys. Rev.* **D77** (2008) 094019.

[28] R. L. Delgado, A. Dobado, D. Espriu, C. Garcia-Garcia, M. J. Herrero, X. Marcano, and J. J. Sanz-Cillero, arXiv:1707.04580 [hep-ph].

[29] A. Pich, I. Rosell, and J. J. Sanz-Cillero, *JHEP* **01** (2014) 157.

[30] **CMS** Collaboration, A. Hinzmann, *PoS* **EPS-HEP2013** (2013) 283.

[31] **CMS** Collaboration, C. Collaboration.

[32] **ATLAS** Collaboration, M. Aaboud *et al.*, arXiv:1708.09638 [hep-ex].

[33] A. Filipuzzi, J. Portoles, and P. Ruiz-Femenia, *PoS* **CD12** (2013) 053.